J Mater Sci (2018) 53:1527–1539

Polymers

Antioxidant electrospun zein nanofibrous web encapsulating quercetin/cyclodextrin inclusion complex

Zeynep Aytac[1], Semran Ipek[2], Engin Durgun[1], and Tamer Uyar[1,*]

[1] *Institute of Materials Science and Nanotechnology, UNAM-National Nanotechnology Research Center, Bilkent University, 06800 Ankara, Turkey*

[2] *Department of Engineering Physics, Istanbul Medeniyet University, 34700 Istanbul, Turkey*

Received: 12 June 2017
Accepted: 14 September 2017
Published online: 10 October 2017

ABSTRACT

Quercetin/gamma-cyclodextrin inclusion complex (quercetin/γ-CD-IC)-encapsulated electrospun zein nanofibers were designed as a quick and an efficient antioxidant nanofibrous material via electrospinning. Structural and thermal analyses along with the solubility enhancement as observed in phase-solubility diagram support the successful formation of the inclusion complexation between quercetin and γ-CD. The molar ratio of quercetin and γ-CD was found 1:1 in quercetin/γ-CD-IC which was confirmed with experimental (phase solubility and ^{1}H-NMR) and computational modeling studies. Computational modeling was also useful to indicate that B orientation is more favorable when quercetin is forming host–guest inclusion complexation with γ-CD from the narrow rim. This result was also consistent with the calculations of the experimental studies performed by ^{1}H-NMR. The successful electrospinning of zein nanofiber encapsulating quercetin/γ-CD-IC (zein-quercetin/γ-CD-IC-NF) yielded bead-free nanofiber morphology having 750 ± 255 nm fiber diameter. For comparative studies, pristine zein nanofibers (zein-NF, 695 ± 290 nm) and zein nanofibers encapsulating quercetin only (zein-quercetin-NF, 750 ± 310 nm) were also electrospun. The antioxidant (AO) characteristics of zein-quercetin/γ-CD-IC-NF were studied by the concentration-dependent AO activity tests.

Introduction

Quercetin (Fig. 1a) is a natural antioxidant due to the functional groups in its molecular structure. The mechanism for antioxidant activity of quercetin is scavenging free radicals through chelating divalent cations, which inhibit some enzymes and protect the DNA damage. The limitations about the therapeutic benefits of quercetin are related with its poor aqueous solubility, absorption, permeability, and oxygen or light-induced decomposition over time [1–3]. Cyclodextrins (CDs) are starch derivatives, non-toxic,

Address correspondence to E-mail: tamer@unam.bilkent.edu.tr

DOI 10.1007/s10853-017-1580-x

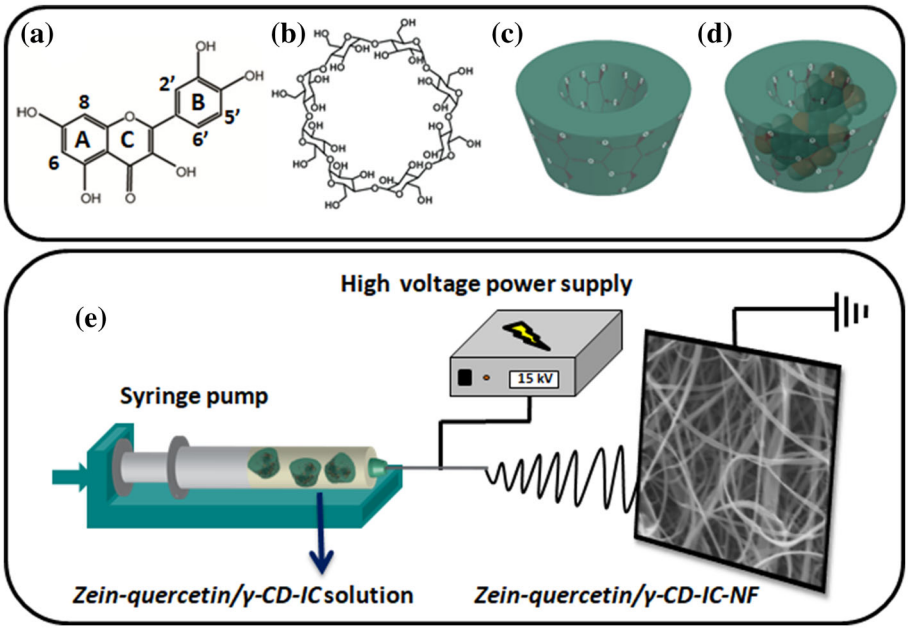

Figure 1 Chemical structure of **a** quercetin and **b** γ-CD; schematic representation of **c** γ-CD and **d** quercetin/γ-CD-IC formation, and **e** electrospinning of nanofibers from zein-quercetin/γ-CD-IC solution.

biodegradable and environmentally benign molecules. CDs are cyclic oligosaccharides and consist of (α-1,4)-linked α-*D*-glucopyranose unit, having molecular structure of macrocycle shape of a hollow truncated cone with somewhat lipophilic central cavity and a hydrophilic outer surface [4]. The most widely used native CDs are named as α-CD (6 units), β-CD (7 units), and γ-CD (8 units) depending on the number of glucopyranose units in the molecular structure [4]. Accordingly, the different size cavity of each CD types enables to form non-covalent inclusion complexes (ICs) with molecules having various sizes/shapes. In addition to molecular size/shape, the polarity matching between the guest molecules and CDs is of importance for the formation of complex in which hydrophobic forces play a significant role [5]. The use of γ-CD (Fig. 1b, c) is sometimes serves as a better choice when compared to α-CD and β-CD, thanks to its wider cavity and higher water solubility and bioavailability, and the absence of side effects on the absorption of nutrients in food products and nutraceutical applications [6]. There are studies in the literature on complexation of quercetin with CDs [7, 8]. In the study of Bergonzi et al. [7], complexation of quercetin was prepared with α-CD, β-CD, and γ-CD by kneading or freeze-drying methods and the solubility enhancement of quercetin was observed in the presence of β-CD. In another study, quercetin was inserted into the cavity of γ-CD by co-precipitation technique and true complexation between quercetin and γ-CD was confirmed by several techniques [8]. Carlotti et al. [9] synthesized a complex of quercetin with methylated β-CD, and this complex exhibited modest improvement in the photostability of quercetin along with enhanced solubility. Complexation of quercetin with β-CD, hydroxypropyl-β-CD, and sulfobutyl ether-β-CD has resulted in solubility and stability improvement as shown in another study [10]. In a recent study of ours, CD-IC of quercetin was encapsulated in polyacrylic acid nanofibers by using electrospinning technique and this nanofibrous web was shown to have quite high antioxidant activity and slow release of quercetin [11].

Electrospinning is a technique to produce nanofibers from various types of materials including polymers, ceramics, composites. One of the known strategy to fabricate functional electrospun nanofibers is to encapsulate active agents (drugs, food additives, antioxidants, antibacterials, and flavor/fragrance, etc.) in the nanofiber matrix [12–16]. It was reported in the studies concerning quercetin-encapsulated electrospun nanofibers that single and core–shell nanofibers could be obtained. Vashisth et al. [2] produced quercetin-encapsulated poly(d,l-lactide-co-glycolide)–poly(ε-caprolactone) nanofibers and investigated the antifungal activity of this nanofiber. In another study conducted by Li et al. [17], quercetin-loaded zein nanoribbons were produced via electrospinning and in vitro dissolution tests were

performed. Thipkaew et al. [18] achieved quercetin-encapsulated electrospun zein nanofibers and showed their effect in the recovery from neuropathy. Li et al. [19] produced fast-dissolving core–shell nanofibers from quercetin/polyvinylpyrrolidone (PVP) solution and PVP/sodium dodecyl sulfate solution in the core and shell, respectively.

In this study, quercetin/γ-cyclodextrin inclusion complex (quercetin/γ-CD-IC) was successfully formed with 1:1 molar ratio of quercetin/γ-CD (Fig. 1d). Phase solubility test, proton nuclear magnetic resonance (^{1}H-NMR), thermogravimetric analysis (TGA), Fourier transform infrared spectrometer (FTIR) and X-ray diffraction (XRD) were employed to characterize quercetin/γ-CD-IC. The computational modeling study was also performed in vacuum and solution (water) for quercetin/γ-CD-IC at 1:1 molar ratio of quercetin/γ-CD. As a next step, quercetin/γ-CD-IC crystals were dispersed in zein solution and then encapsulated into zein nanofiber matrix by using electrospinning technique (Fig. 1e). For the comparative studies, pristine zein nanofibers (zein-NF) and zein nanofibers encapsulating quercetin only (zein-quercetin-NF) were also electrospun. The morphology, structural and thermal analyses of zein nanofibers (zein-NF, zein-quercetin-NF and zein-quercetin/γ-CD-IC-NF) were investigated by scanning electron microscopy (SEM), FTIR, XRD and TGA, respectively. Antioxidant (AO) activity of zein-NF, zein-quercetin-NF and zein-quercetin/γ-CD-IC-NF was determined by concentration-dependent 2,2-diphenyl-1-picrylhydrazyl (DPPH) radical scavenging assay.

Experimental

Materials

Zein from maize (Sigma-Aldrich), quercetin (≥ 95%, Sigma-Aldrich), ethanol (99.8%, Sigma-Aldrich), methanol (extra pure, Sigma-Aldrich), deuterated dimethylsulfoxide (DMSO-d6, deuteration degree min 99.8% for NMR spectroscopy, Merck), 2,2-diphenyl-1-picrylhydrazyl (DPPH, Sigma-Aldrich) were purchased and used as received without any further purification. Gamma-cyclodextrin (γ-CD) was kindly donated by Wacker Chemie AG (Germany). The water used in the experiments was distilled–deionized from a Millipore Milli-Q ultrapure water system.

Preparation of the quercetin/γ-CD-IC

The solid inclusion complex (IC) between quercetin and γ-CD (quercetin/γ-CD-IC) was synthesized by using the freeze-drying method. In a typical quercetin/γ-CD-IC formation studies, 0.5 g of γ-CD was dissolved in water (10 mL) and 0.12 g of quercetin (equivalent to 1:1 molar ratio) was directly added to the solution. The solution was stirred at room temperature (RT) at 500 rpm for 12 h and frozen at −80 °C for 24 h. Finally, solid complex was obtained by drying the solution in lyophilizer (Labconco, FreeZone 4.5) for 48 h. Finally, quercetin/γ-CD-IC crystals in the form of yellowish powder were obtained. As a control sample, physical mixture of quercetin/γ-CD (quercetin/γ-CD-PM) was prepared by mixing quercetin and γ-CD (equivalent to 1:1 molar ratio) simply in solid state as a powder form.

Preparation of zein solutions for electrospinning

Zein nanofibers (zein-NF), zein nanofibers encapsulating quercetin only (zein-quercetin-NF), and quercetin/γ-CD-IC-encapsulated zein nanofibers (zein-quercetin/γ-CD-IC-NF) were produced via electrospinning. The 35% (w/v) zein solution was prepared in ethanol/water (8:2, v/v) at RT for the electrospinning of zein-NF. For zein-quercetin-NF, quercetin solution (5%, w/w, with respect to polymer) in ethanol/water (8:2, v/v) at RT was prepared and then 35% (w/v) zein solution was added into that quercetin solution for the electrospinning process. For the electrospinning of zein-quercetin/γ-CD-IC-NF, quercetin/γ-CD-IC (corresponding to 5% (w/w) quercetin with respect to zein) was dispersed in ethanol/water (8:2, v/v) at RT; next, 35% (w/v) zein was added to this quercetin/γ-CD-IC dispersion and the suspension was stirred for 2 h before electrospinning. Table 2 summarizes the compositions of the zein, zein-quercetin, and zein-quercetin/γ-CD-IC solutions.

Electrospinning

The electrospinning setup is composed of a syringe pump (KD Scientific, KDS101) and high voltage–power supply (AU Series, Matsusada Precision, Inc.). Zein-NF, zein-quercetin-NF, and zein-quercetin/γ-CD-IC-NF were produced from zein, zein-quercetin,

and zein-quercetin/γ-CD-IC solutions at a flow rate of 1 mL/h and applying a voltage of 15 kV, respectively. The distance between the needle (needle i.d. = 0.9 mm) was 10 cm, and a rectangular metal plate covered with aluminum foil was used as a collector. The electrospinning was performed at 25 °C and 18% relative humidity.

Characterizations and measurements

Phase solubility diagram was obtained by adding excess amount of quercetin in varying concentration of aqueous γ-CD solutions. The resulting solutions were stirred 24 h at RT, and then they were filtered using membrane filter (M&Nagel RC 0.45/25). Finally, the absorbance of the solutions was recorded at 375 nm by UV–Vis spectroscopy (Varian, Cary 100). The experiments were carried out in triplicate, and each data point is the average of three determinations. The stability constant (Ks) of the quercetin/γ-CD-IC system was calculated based on the phase solubility diagram according to the following equation:

$$K_s = \text{slope}/S_0(1 - \text{slope}) \quad (1)$$

where S_0 is the intrinsic solubility of quercetin (quercetin solubility in the absence of CD).

Proton nuclear magnetic resonance (^{1}H-NMR) spectrum of quercetin/γ-CD-IC was obtained by dissolving the solid powder in DMSO-d6 (Bruker DPX-400). The integration of the peaks corresponding to the protons of quercetin and γ-CD was calculated by using Mestrenova software.

The infrared spectra of pure quercetin, pristine γ-CD, quercetin/γ-CD-IC, quercetin/γ-CD-PM, zein-NF, zein-quercetin-NF, zein-quercetin/γ-CD-IC-NF were obtained by using a Fourier transform infrared spectrometer (FTIR) (Bruker-VERTEX 70). The scans (64 scans) were recorded between 4000 and 400 cm^{-1} at resolution of 4 cm^{-1}.The crystalline structure of quercetin, γ-CD, quercetin/γ-CD-IC, quercetin/γ-CD-PM, zein-NF, zein-quercetin-NF, and zein-quercetin/γ-CD-IC-NF was investigated via X-ray diffraction (XRD) (PANalytical X'Pert powder diffractometer) using Cu Kα radiation in a powder diffraction configuration.

The thermal properties of quercetin, γ-CD, quercetin/γ-CD-IC, quercetin/γ-CD-PM, zein-NF, zein-quercetin-NF, and zein-quercetin/γ-CD-IC-NF were analyzed using thermogravimetric analysis (TGA, TA Q500, USA) by heating the samples from RT up to 600 °C at a rate of 20 °C/min under nitrogen atmosphere.

Scanning electron microscopy (SEM, FEI-Quanta 200 FEG) was employed to examine the morphology of zein-NF, zein-quercetin-NF, and zein-quercetin/γ-CD-IC-NF. The nanofibrous web samples mounted on the metal stubs using a double-sided adhesive tape were coated with Au/Pd layer (~5 nm) (PECS-682) prior to SEM imaging in order to minimize the charging. Average fiber diameter (AFD) of the nanofibers was calculated on SEM images ($n \geq 100$, different locations of the samples), and the results were reported as average ± standard deviation.

Antioxidant (AO) activity of zein-NF, zein-quercetin-NF, and zein-quercetin/γ-CD-IC-NF was determined according to DPPH radical scavenging assay by varying the concentration of the samples. The nanofibrous webs of zein-NF (4.5 mg) and zein-quercetin-NF (3.8 mg) and zein-quercetin/γ-CD-IC-NF (4.5 mg) having equivalent amount of quercetin (0.18 mg) were immersed separately in 3 mL of methanol/water (1:1, v/v) and stirred for 30 min. Then, these solutions were diluted starting from 60 to 6, 1.2, and 0.6 ppm and added separately into 2 mL of 10^{-4} M DPPH solution which was prepared in methanol/water (1:1, v/v). The resulting solutions were incubated at RT for 1 h, and finally absorbance of the solutions was measured by UV–Vis spectroscopy (Varian, Cary 100) at 521 nm.

AO activity (%) was calculated based on the following equation:

$$\text{AO activity } (\%) = \left(A_{\text{control}} - A_{\text{sample}}\right)/A_{\text{control}} * 100 \quad (2)$$

where A_{control} and A_{sample} represent the absorbance values of control DPPH solution and DPPH solution with nanofibers, respectively.

Computational method

The ab initio structural optimization calculations based on density functional theory (DFT) [20, 21] were performed by using the Vienna Ab initio simulation package [22, 23]. The exchange–correlation was approximated by generalized gradient approximation using Perdew–Burke–Ernzerhof functional [24]. The van der Waals correction was also taken into account for better characterization of the intermolecular interactions [25]. The projector augmented-wave

method (PAW) [26] was utilized for pseudopotentials of all elements with a plane-wave basis set having a kinetic energy cutoff of 520 eV. The initial structure of γ-CD was obtained from Cambridge Structural Database [27]. All the structures including inclusion complexes were optimized by using the conjugate gradient algorithm without any constraints by setting convergence criteria on the total energy and force to 10^{-4} eV and 10^{-2} eV/Å, respectively. The effect of water as a solvent on the formation of inclusion complex has been examined by using implicit solvent model [28], which also includes dispersive interactions. This model splits the system into an explicit part (solute), which is treated quantum mechanically, and an implicit part (solvent), which is treated as a continuum [29]. The intermolecular interactions between water molecules are gathered from continuum dielectric description of the solvent [30, 31].

Results and discussion

Phase-solubility study

Phase solubility diagram of quercetin/γ-CD-IC system in aqueous solution is given in Fig. 2. The linear increment of the absorbance (A_L type) of quercetin with increasing amount of γ-CD indicates the solubility of quercetin is improved up to 6 mM of CD. This result also supports 1:1 complex formation between quercetin and γ-CD. Stability constant (K_s) of the quercetin/γ-CD system was also calculated as 0.91 M^{-1}. The calculated K_s is quite low as compared to our previously published result on quercetin/β-CD-IC (3345 M^{-1}) [11] and shows that the interaction is weak between quercetin and γ-CD. The lower Ks value for quercetin/γ-CD-IC is possibly because of the wider cavity size of γ-CD compared to β-CD [4].

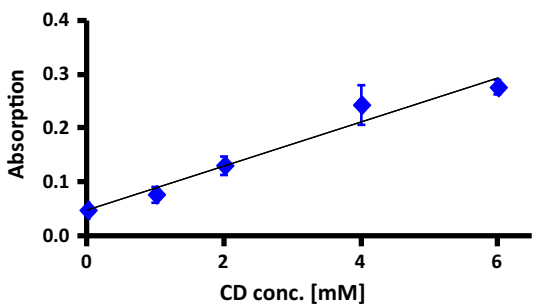

Figure 2 Phase solubility diagram of quercetin/γ-CD system in aqueous solution ($n = 3$).

The molar ratio of quercetin/γ-CD-IC

The molar ratio of quercetin and γ-CD in quercetin/γ-CD-IC was calculated by the proportion of characteristic proton peaks of each compound in the proton nuclear magnetic resonance (^{1}H-NMR) spectra. As seen from Fig. 3, selected proton peaks of quercetin (6.9 ppm) and γ-CD (4.5 ppm) were used to determine the molar ratio which was calculated as 1:1 for quercetin/γ-CD. Similar to phase solubility result, the ^{1}H-NMR study showed that 1:1 molar ratio of quercetin/γ-CD was obtained once the complexation has been formed in the form of solid crystals of quercetin/γ-CD-IC.

Chemical shift variation of guest and host molecules could give information about the orientation of the guest molecule in the cavity of CD and the rim of CD while guest molecule is entering the cavity. Since inclusion of a hydrophobic guest molecule into the cavity causes a shielding effect especially on the inner protons of CD, H-3 and H-5 which are located close to the wider and narrower rim, respectively [32]. The chemical shifts of quercetin, γ-CD, and quercetin/γ-CD-IC are given in Table 1. H-3 and H-5 protons of γ-CD displayed chemical shifts at 3.540 and 3.595 ppm; however, after the formation of the complex H-3 proton shifted 0.005 ppm, whereas H-5 proton shifted 0.006 ppm, respectively. The slightly higher chemical shift observed in H-5 proton might show that quercetin prefers to enter to the cavity of γ-CD from the narrower rim of the cavity. In addition, the higher chemical shift seen in 5′, 6′, and 2′ protons which are located in the B ring of quercetin as shown in Fig. 1 indicated the B orientation is more favorable

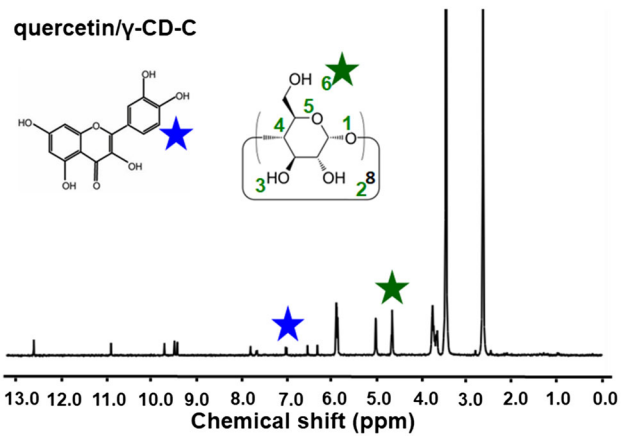

Figure 3 ^{1}H-NMR spectra of quercetin/γ-CD-IC dissolved in DMSO-d6.

Table 1 Variation of the ^{1}H NMR chemical shifts (δ/ppm) of quercetin, γ-CD, and quercetin/γ-CD-IC protons in free and complex states determined in DMSO-d6 at 25 °C

	δ_{free}	$\delta_{complex}$	$\Delta\delta$
6 of quercetin	6.186	6.185	0.001
8 of quercetin	6.405	6.405	0.000
5′ of quercetin	6.875	6.869	0.006
6′ of quercetin	7.528	7.522	0.006
2′ of quercetin	7.677	7.670	0.007
H-3 of γ-CD	3.540	3.545	0.005
H-5 of γ-CD	3.595	3.601	0.006

for the complex formed between quercetin and γ-CD. The chemical shift results are in the agreement with the computational modeling study.

Structural characterization of quercetin/γ-CD-IC and nanofibers

The chemical structure of quercetin, γ-CD, quercetin/γ-CD-IC, quercetin/γ-CD-PM, zein-NF, zein-quercetin-NF, zein-quercetin/γ-CD-IC-NF was investigated by Fourier transform infrared spectroscopy (FTIR). The typical absorption bands of γ-CD are observed at around 3401, 2925, 1638, 1159, 1082, and 1028 cm^{-1} corresponding to O–H stretching, C–H stretching, H–OH bending, asymmetric stretching vibration of C–O–C glycosidic bridge, C–O stretching vibration, and C–C stretching vibration, respectively. Quercetin exhibited characteristic bands and peaks at around 3429–3238 cm^{-1} (O–H), 1674 cm^{-1} (C=O), 1616 cm^{-1} (C=C), 1359 cm^{-1} (C–OH), and 1245 cm^{-1} (C–O–C) [33]. The band at around 3388 cm^{-1} in FTIR spectrum of quercetin/γ-CD-IC might be attributed to the O–H bending of both γ-CD and quercetin. The peaks observed at 1654, 1614, 1363, and 1242 cm^{-1} show the presence of quercetin in quercetin/γ-CD-IC; slight shifts seen in these peaks are the confirmation of an interaction between quercetin and γ-CD. Quercetin/γ-CD-IC has also displayed shifted peaks at around 2925, 1159, 1080, and 1026 cm^{-1} which correspond to the peaks of γ-CD and confirm the existence of an interaction between quercetin and γ-CD. The typical peaks of quercetin were seen at 1674, 1618, 1359, 1245 cm^{-1}, whereas the peaks at 2925, 1161, 1082, and 1028 cm^{-1} are attributed to γ-CD in quercetin/γ-CD-PM. As it is clear that the FTIR peaks belong to quercetin and γ-CD were shifted more in quercetin/γ-CD-IC as compared to quercetin/γ-CD-PM which strongly suggest the inclusion complexation between quercetin and γ-CD for quercetin/γ-CD-IC sample. Furthermore, the intensity of the quercetin peaks was reduced for quercetin/γ-CD-IC as compared to quercetin/γ-CD-PM which also indicates the presence of inclusion complexation between quercetin and γ-CD (Fig. 4a).

Zein-NF exhibited characteristic absorption bands of zein at around 1656 cm^{-1} (amide I) and 1540 cm^{-1} (amide II) [34]. Zein-quercetin-NF and zein-quercetin/γ-CD-IC-NF displayed the characteristic peaks of zein at 1652 and 1656 cm^{-1} for amide I and 1541 and 1541 cm^{-1} for amide II, respectively. However, due to the overlapping of the intense peaks of zein, it is not easy to clearly identify the peaks of quercetin in FTIR spectra of both zein-quercetin-NF and zein-quercetin/γ-CD-IC-NF. The peaks of γ-CD seen at 1161 and 1028 cm^{-1} corresponds to the asymmetric stretching vibration of C–O–C glycosidic bridge and C–C stretching vibration of γ-CD in the spectrum of zein-quercetin/γ-CD-IC-NF, respectively. The slight shift observed in the peak of γ-CD (1159 cm^{-1} shift to 1161 cm^{-1}) might be due to the presence of an interaction between γ-CD and zein in the zein-quercetin/γ-CD-IC-NF matrix (Fig. 4b).

X-ray diffraction (XRD) is a widely used method to analyze the complex formation with CDs and the guest molecules [11, 35, 36]. Since it is a known fact that the crystalline peaks of the guest molecules cannot be observed due to the CD cavities hindering the formation of crystalline structures [11, 35, 36]. XRD patterns of quercetin, γ-CD, quercetin/γ-CD-IC, and physical mixture of quercetin/γ-CD (quercetin/γ-CD-PM) are shown in Fig. 5a, whereas XRD patterns of zein-NF, zein-quercetin-NF, and zein-quercetin/γ-CD-IC-NF are given in Fig. 5b. The crystalline peaks of quercetin (10.2°, 11.0°, 13.6°, 16.6°, 18.0°, 21.9°, 23.4°, 24.5°, 25.3°, 25.8°, 26.2°, 27.1°, 27.8°) and cage-type crystalline peaks of γ-CD (5.4°, 12.5°, 15.7°, 16.7°, 19.1°, 21.9°) disappeared in the XRD pattern of quercetin/γ-CD-IC. Moreover, new peaks with a major peak at 6° were raised corresponding to the channel-type crystalline hexagonal packing of γ-CD molecules. The hexagonal packing of γ-CD in the crystal structure of the styrene/γ-CD-IC after vacuum-drying was previously reported in the study of Uyar et al. [37]. Here, the diffraction pattern of quercetin/γ-CD-IC obtained by freeze-drying has shown the channel structure of hexagonal packing [37], which confirms the complex formation between

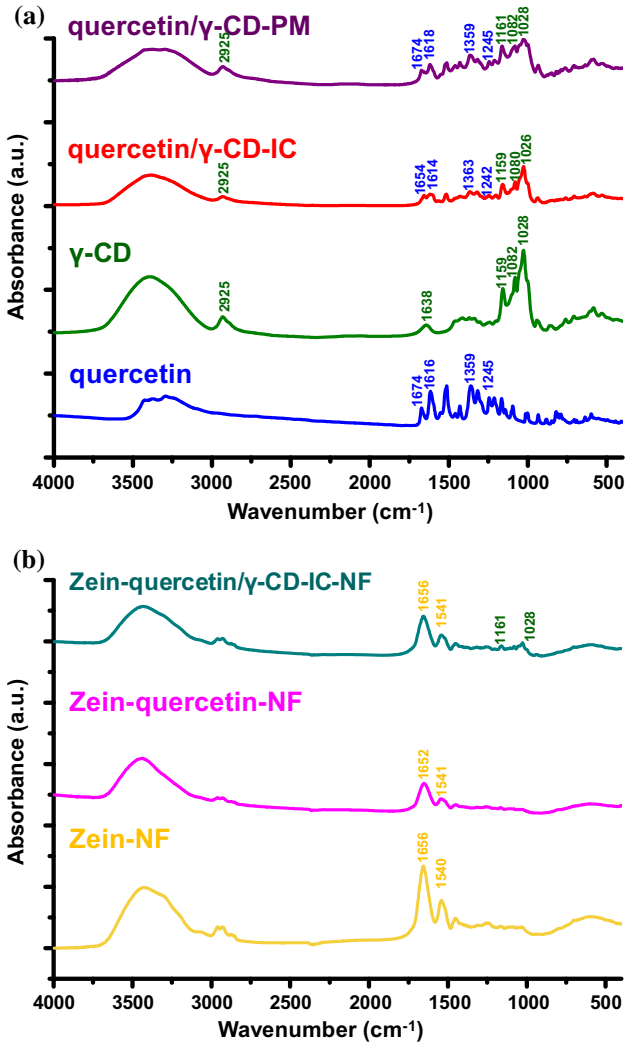

Figure 4 FTIR spectra of **a** quercetin, γ-CD, quercetin/γ-CD-IC, and quercetin/γ-CD-PM; **b** zein-NF, zein-quercetin-NF, and zein-quercetin/γ-CD-IC-NF.

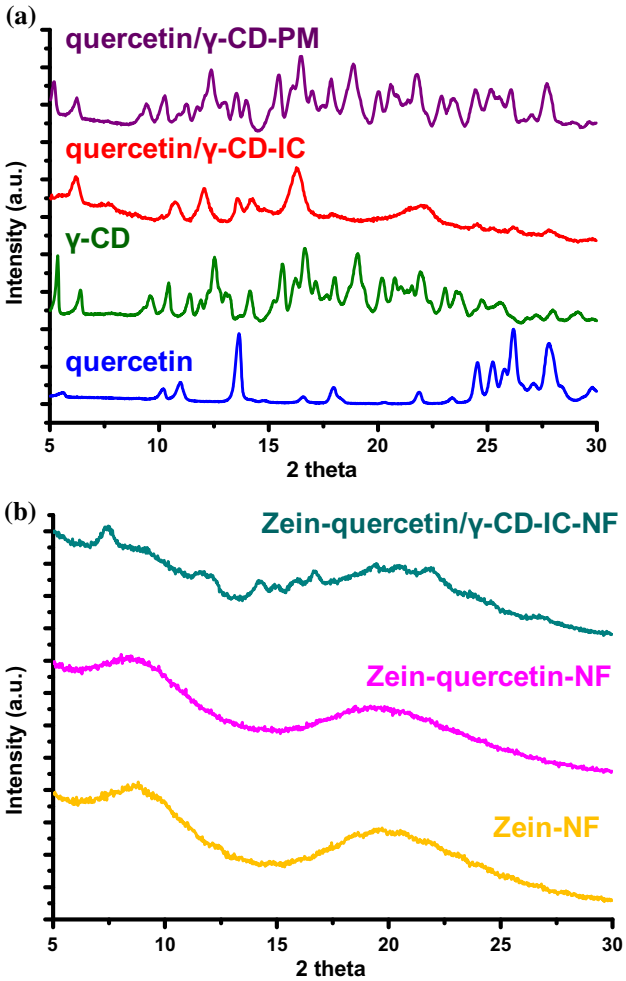

Figure 5 XRD patterns of **a** quercetin, γ-CD, quercetin/γ-CD-IC, and quercetin/γ-CD-PM; **b** zein-NF, zein- quercetin-NF, and zein-quercetin/γ-CD-IC-NF.

quercetin and γ-CD [35]. In contrast to quercetin/γ-CD-IC, quercetin/γ-CD-PM exhibited the peaks of quercetin especially in the 2θ range of 5° and 25°–30° and most of the peaks belong to the cage-type crystal packing of γ-CD. Zein-NF and zein-quercetin-NF exhibited broad peaks in XRD patterns, and the disappearance of the crystalline peaks of quercetin might be due to the amorphous distribution of the compounds in zein-quercetin-NF. However, zein-quercetin/γ-CD-IC-NF exhibited the characteristic tetragonal diffraction peaks with a major peak at 7.5° and minor peaks at 14°, 15°, 16°, 17°, and 22° of channel-type packing of γ-CD [37] and this result shows the presence of quercetin/γ-CD-IC crystals in the zein nanofiber matrix. These data are similar to previous study where we have also observed channel-type packing of γ-CD for electrospun polyvinyl alcohol (PVA) nanofibers encapsulating geraniol/γ-CD-IC [38].

Thermal analysis of quercetin/γ-CD-IC and nanofibers

The thermal stability of quercetin, γ-CD, quercetin/γ-CD-IC, quercetin/γ-CD-PM, zein-NF, zein-quercetin-NF, and zein-quercetin/γ-CD-IC-NF was further investigated by thermal gravimetric analysis (TGA), and the results are given in Fig. 6a, b. Thermal degradation of quercetin is observed between 245 and 390 °C. γ-CD exhibited two steps of weight loss, the first one, which is 100 °C corresponding to water loss in the cavity (7.6%), and the second weight loss

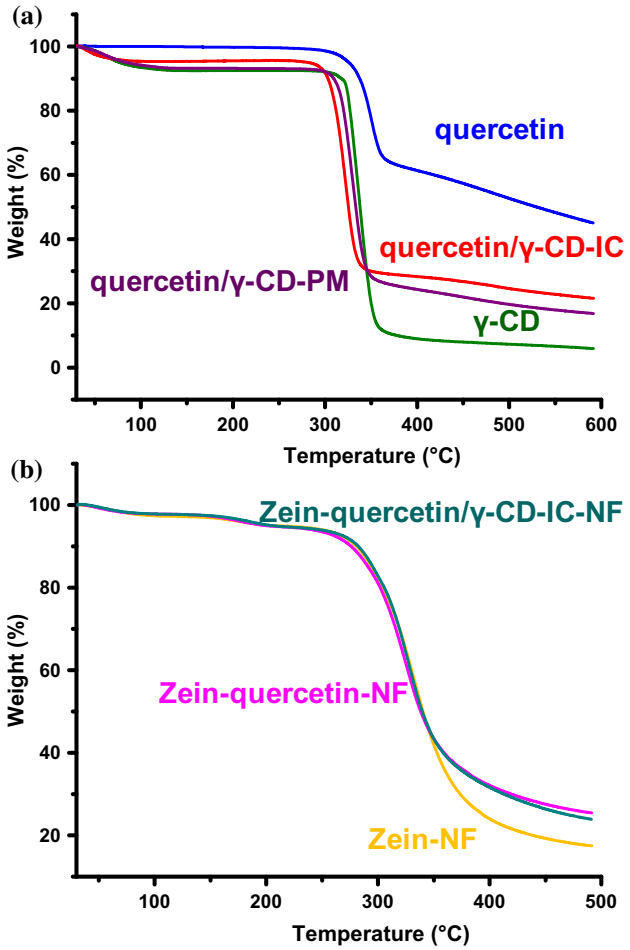

Figure 6 TGA thermograms of **a** quercetin, γ-CD, quercetin/γ-CD-IC, and quercetin/γ-CD-PM; **b** zein-NF, zein-quercetin-NF, and zein-quercetin/γ-CD-IC-NF.

which is between 270 and 425 °C attributed to the main thermal degradation of γ-CD. The water loss of quercetin/γ-CD-IC is observed below 90 °C as 4.7%. However, because of the overlapping in the main thermal degradation of quercetin and γ-CD in quercetin/γ-CD-IC between 250 and 400 °C, the amount of quercetin in quercetin/γ-CD-IC could not be calculated from TGA data. Quercetin/γ-CD-PM possesses two stage of weight loss below 140 °C and at 260–400 °C. The first weight loss belongs to the water loss, and it is around 6.7%, which is more than the amount of water present in the quercetin/γ-CD-IC. This is another support of complex formation between quercetin and γ-CD in quercetin/γ-CD-IC. Because when complex is formed, the guest molecule replaces the water in the cavity. For instance, in our previous report we showed that HPβCD/triclosan-IC nanofibers had lower water content owing to the complex formed between HPβCD and triclosan as compared to pristine HPβCD nanofibers [39]. In addition, the thermal stability of quercetin did not change by complexation. Similar results were reported in a study of Koontz et al. [8] in which the thermal stability of quercetin did not alter by complexation with γ-CD.

Zein-NF has shown three steps of weight loss: below 110 °C; at 130–210 °C, and 220–490 °C. The first weight loss up to 110 °C is due to water and volatile components, whereas the weight losses after 130 °C correspond to the protein degradation which is observed mostly after 220 °C. This result is in agreement with the previously published literature data by Neo et al. [40]. The weight loss of zein-quercetin-NF was also occurred in three steps, below 110 °C, at 120–220 °C, and 220–490 °C corresponding to water, zein, and quercetin and zein, respectively. The amount of quercetin in the nanofibers could not be determined because of the overlapping in the thermal degradation of quercetin and zein. As regards to zein-quercetin/γ-CD-IC-NF, three steps of weight loss were seen below 110 °C (water loss), at 130–220 °C (zein and quercetin), and 220–490 °C (quercetin, γ-CD, and zein). Therefore, because of the overlapping in the thermal decomposition of quercetin, γ-CD, and zein, it was not possible to determine the amount of quercetin in the nanofibers as well.

Molecular modeling of quercetin/γ-CD-IC

The inclusion complex formation depends on the interactions between the guest molecule and the CD. These interactions are altered by the environment conditions, thus the type of the solvent can affect the complexation reaction dynamics and the strength of the complexation. Therefore, to elucidate the complexation of quercetin within γ-CD, we carried out structural optimization of quercetin molecule, γ-CD, and their ICs in vacuum, followed by optimizations in water as a solvent environment. Single quercetin molecule is introduced into the narrow rim of γ-CD cavity with two possible orientations at 1:1 stoichiometry, labeled as A and B (Fig. 7a, b) at various sites to form IC. The most favorable geometry of quercetin/γ-CD-IC in 1:1 stoichiometry is determined by calculating the total energy of the system for these possible configurations. The complexation formation at the center of the CD cavity has been found

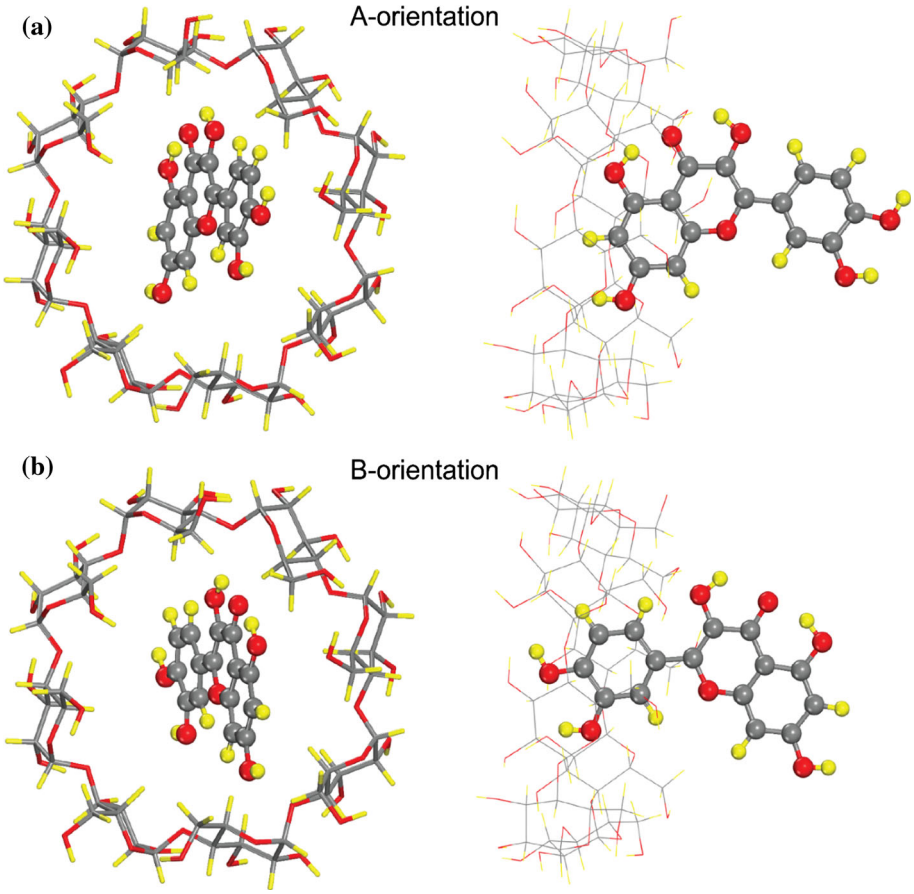

Figure 7 Top and side view of quercetin/γ-CD-IC for **a** A orientation and **b** B orientation at 1.0:1.0 stoichiometry. Gray, red, and yellow spheres represent carbon, oxygen, and hydrogen atoms, respectively.

energetically more favorable compared to other possible sites within CD cavity.

Once the lowest energy configuration is obtained, the complexation energy (E_{comp}) can be calculated as

$$E_{comp} = E_{(CD)} + E_{(guest)} - E_{(IC)} \quad (3)$$

where $E_{(CD)}$, $E_{(guest)}$, and $E_{(IC)}$ is the total energy (in vacuum or solvent) of γ-CD; guest molecule (quercetin); and their IC for 1:1 stoichiometry, respectively. For the lowest energy configuration in A and B orientation as shown in Fig. 7a, b, E_{comp} is found to be 3.9 and 7.8 kcal/mol in vacuum and 6.9 and 9.2 kcal/mol in solvent, respectively. Positive E_{comp} indicates that IC forms seamlessly for both in vacuum and water; however, E_{comp} in water is higher indicating a stronger interaction and more favorable complexation in aqueous environment. Our calculations also indicate that B orientation of quercetin within γ-CD cavity is favored when compared to A orientation. In our previously published study [11] on quercetin and β-CD, we have observed that the energy values calculated for A and B orientation at 1:1 molar ratio in vacuum was comparable to each other; thus, the results suggested that there is no significant preference in the orientation. As a conclusion, computational modeling results confirmed the formation of the complex with the B orientation of quercetin from the narrower rim of the γ-CD consistent with the chemical shift results obtained from ^{1}H-NMR.

Additionally, the solvation energies of ICs in water are calculated to figure out the solubility trends. The solvation energy (E_{solv}) of ICs in water can be calculated as

$$E_{solv} = E_{(IC)solvent} - E_{(IC)vacuum} \quad (4)$$

where $E_{(IC)solvent} - E_{(IC)vacuum}$ is the total energy of quercetin/γ-CD-IC in water and vacuum for the lowest energy configurations, respectively. The calculated E_{solv} are − 91.5, − 74.2 and − 12.2 kcal/mol for IC, γ-CD and single quercetin molecule, respectively. These results indicate that IC formation makes the whole system more soluble under water compared to their bare cases. The results are in agreement with the findings of experimental studies in which 1:1 complex formation and improved aqueous solubility

was confirmed by ^{1}H-NMR and phase solubility test, respectively.

Morphology analyses of nanofibers

The morphology of zein-NF, zein-quercetin-NF, and zein-quercetin/γ-CD-IC-NF was investigated using scanning electron microscopy (SEM). The representative SEM images of the nanofibrous webs along with fiber distributions are given in Fig. 8a–c. Average fiber diameter (AFD) was calculated from SEM images as 685 ± 290, 750 ± 310, and 750 ± 255 nm for zein-NF, zein-quercetin-NF, and zein-quercetin/γ-CD-IC-NF, respectively. All nanofibers exhibited bead-free morphology, but there is slight difference in the AFD of nanofibers. The AFD of zein-NF increased when quercetin or quercetin/γ-CD-IC incorporated into zein nanofibers, and yielding thicker fibers is possibly due to the increment of the viscosity and reduction in the conductivity causing less stretching of the jet [41] as compared to zein solution (Table 2).

Antioxidant activity

Antioxidant (AO) activity of zein-NF, zein-quercetin-NF, and zein-quercetin/γ-CD-IC-NF was investigated by 2,2-diphenyl-1-picrylhydrazyl (DPPH) radical scavenging assay, and the results are given along with the photographs in Fig. 9a, b. AO activity of zein-NF, zein- quercetin-NF, and zein-quercetin/γ-CD-IC-NF were determined as 30 ± 5, 43 ± 5, and 44 ± 7% when quercetin concentration was 0.6 ppm

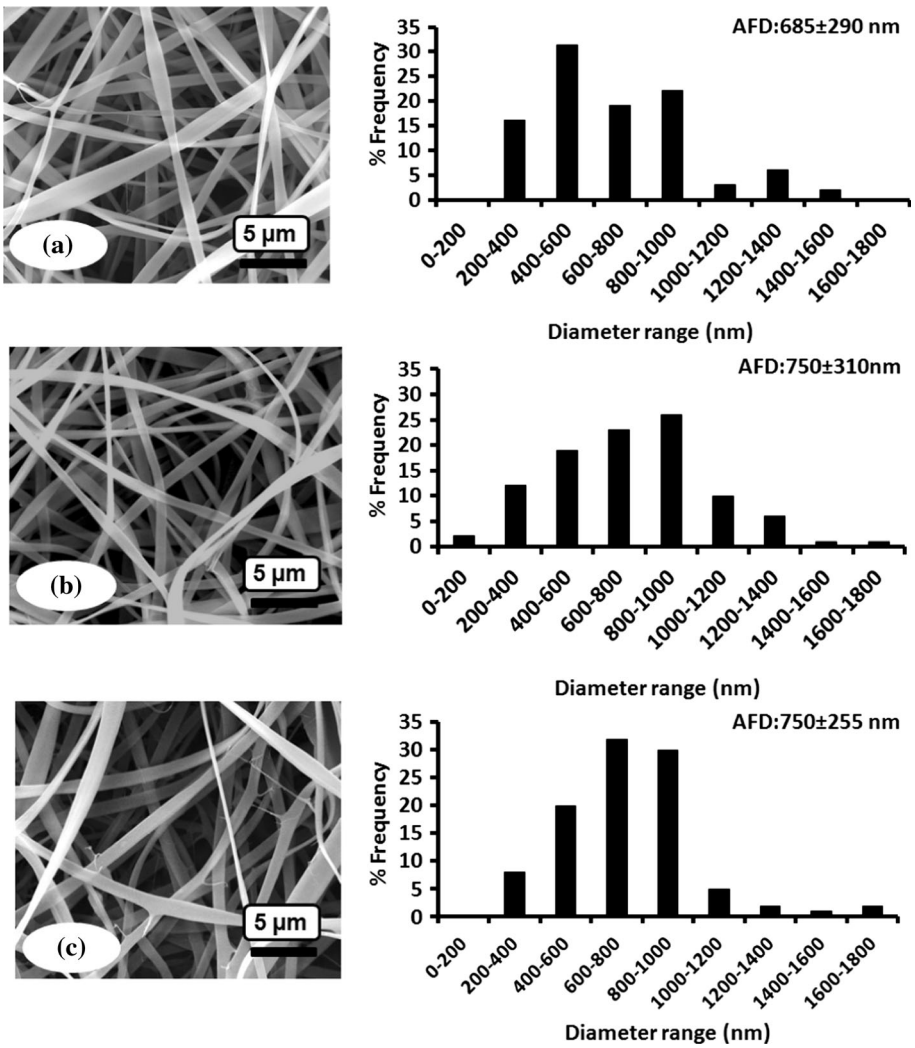

Figure 8 Representative SEM images and fiber diameter distributions with average fiber diameter (AFD) of electrospun nanofibers obtained from the solutions of **a** zein, **b** zein-quercetin, and **c** zein-quercetin/γ-CD-IC.

Table 2 Properties of the solutions used for electrospinning and morphological characteristics of the resulting nanofibers

Solutions	% zein[a] (w/v)	% γ-CD[b] (w/w)	% quercetin[b] (w/w)	Viscosity (Pa·s)	Conductivity (μS/cm)	Average fiber diameter (nm)
Zein	35	–	–	0.12	1200	685 ± 290
Zein-quercetin	35	–	5	0.24	1100	750 ± 310
Zein/quercetin/γ-CD-IC	35	21	5	0.36	1100	750 ± 255

[a]With respect to solvent (ethanol/water, 8:2)

[b]With respect to polymer (zein)

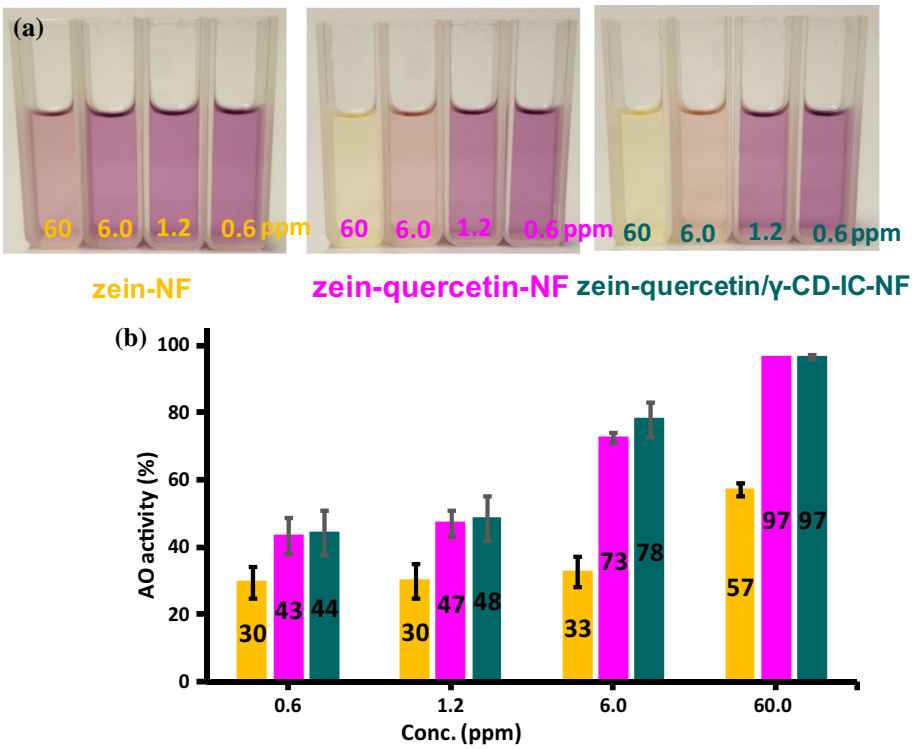

Figure 9 **a** Photographs of the DPPH solutions in which zein-NF, zein-quercetin-NF, and zein-quercetin/γ-CD-IC-NF were immersed with respect to concentration, **b** concentration-dependent AO activity (%) of zein-NF, zein-quercetin-NF, and zein-quercetin/γ-CD-IC-NF.

in the nanofibers, whereas AO activity of zein-NF, zein-quercetin-NF, and zein-quercetin/γ-CD-IC-NF was 57 ± 2, 97 ± 0, and 97 ± 1% when the concentration of quercetin was increased to 60 ppm in the nanofibers, respectively. Efficient concentration (EC50) is defined as the amount of AO compound necessary to decrease DPPH concentration by 50% [42], and lower EC50 is the indication of higher free radical scavenging capability of the compounds. EC50 of zein-NF was close to 60 ppm, and EC50 of both zein-quercetin-NF and zein-quercetin/γ-CD-IC-NF is slightly higher than 1.2 ppm. The photographs shown in Fig. 9a are coherent with the AO activity (%) of nanofibers. The color change depending on the concentration of quercetin in the nanofibers is clearly visible in the photographs of zein-quercetin-NF and zein-quercetin/γ-CD-IC-NF. The purple color of DPPH solution did not change much up to 1.2 ppm, but the color turned into yellow when the concentration reaches to 60 ppm. However, the characteristic purple color of DPPH solution in which zein-NF was immersed did not turn into yellow even at the highest concentration. Briefly, quercetin preserved its bioactivity after incorporation directly in the free form or in the form of CD-IC into zein nanofibers. Moreover, complex formation did not affect the antioxidant activity of quercetin when it is in the CD cavity. This might be due to the high solubility of

quercetin in the test medium which facilitates the release of quercetin from the γ-CD cavity.

Conclusion

Here, quercetin and quercetin/γ-CD-IC-encapsulated electrospun zein nanofibers were successfully obtained by electrospinning technique. First of all, quercetin/γ-CD-IC was prepared by using quercetin and γ-CD at 1:1 molar ratio. The 1:1 molar ratio of quercetin/γ-CD was experimentally confirmed using ^{1}H-NMR technique and phase solubility diagram, and theoretically confirmed by computational modeling. By computational modeling studies, the most favorable quercetin orientation was also determined while making complex with γ-CD in aqueous medium. It was calculated that B orientation is more favorable than A orientation of quercetin and water-solubility improvement of quercetin was also confirmed theoretically which was also supported experimentally by phase solubility test. As a next step, quercetin/γ-CD-IC was encapsulated into zein solution to produce nanofibers. Pristine zein nanofibers and zein nanofibers encapsulating quercetin only (without γ-CD) were also electrospun for comparative studies. According to the findings of AO activity test, quercetin/γ-CD-IC incorporated zein nanofibers exhibited quite high, efficient, and quick AO activity. In brief, encapsulation of antioxidant agents such as quercetin/CD-IC systems into electrospun nanofibrous matrix can be a very practical approach to achieve enhanced water solubility and stability for these active agents. Hence, these nanofibrous webs encapsulation CD-IC of active agents could find certain applications in food, food packaging, pharmaceuticals and healthcare, etc.

Acknowledgements

Dr. Uyar acknowledges The Scientific and Technological Research Council of Turkey (TUBITAK)-Turkey (Project # 111M459) for funding this research. Dr. Uyar and Dr. Durgun acknowledge The Turkish Academy of Sciences-Outstanding Young Scientists Award Program (TUBA-GEBIP) for partial funding of the research. Z. Aytac thanks to TUBITAK-BIDEB and TUBITAK (project # 111M459) for the PhD scholarship.

References

[1] Aceituno-Medina M, Mendoza S, Rodríguez BA, Lagaron JM, López-Rubio A (2015) Improved antioxidant capacity of quercetin and ferulic acid during in vitro digestion through encapsulation within food-grade electrospun fibers. J Funct Foods 12:332–341

[2] Vashisth P, Nikhil K, Pemmaraju SC, Pruthi PA, Mallick V, Singh H, Patel A, Mishra NC, Singh RP, Pruthi V (2013) Antibiofilm activity of quercetin-encapsulated cytocompatible nanofibers against Candida albicans. J Bioact Compat Polym 28(6):652–665

[3] Xing ZC, Meng W, Yuan J, Moon S, Jeong Y, Kang IK (2012) In vitro assessment of antibacterial activity and cytocompatibility of quercetin-containing PLGA nanofibrous scaffolds for tissue engineering. J Nanomater 202608, 7

[4] Szejtli J (1998) Introduction and general overview of cyclodextrin chemistry. Chem Rev 98(5):1743–1754

[5] Rekharsky MV, Inoue Y (1998) Complexation thermodynamics of cyclodextrins. Chem Rev 98(5):1875–1918

[6] Li Z, Wang M, Wang F, Gu Z, Du G, Wu J, Chen J (2007) γ-Cyclodextrin: a review on enzymatic production and applications. Appl Microbiol Biotechnol 77(2):245–255

[7] Bergonzi MC, Bilia AR, Di Bari L, Mazzi G, Vincieri FF (2007) Studies on the interactions between some flavonols and cyclodextrins. Bioorg Med Chem Lett 17(21):5744–5748

[8] Koontz JL, Marcy JE, O'Keefe SF, Duncan SE (2009) Cyclodextrin inclusion complex formation and solid-state characterization of the natural antioxidants α-tocopherol and quercetin. J Agric Food Chem 57(4):1162–1171

[9] Carlotti ME, Sapino S, Ugazio E, Caron G (2011) On the complexation of quercetin with methyl-β-cyclodextrin: photostability and antioxidant studies. J Incl Phenom Macrocycl Chem 70(1–2):81–90

[10] Zheng Y, Haworth IS, Zuo Z, Chow MS, Chow AH (2005) Physicochemical and structural characterization of quercetin-β-cyclodextrin complexes. J Pharm Sci 94(5):1079–1089

[11] Aytac Z, Kusku SI, Durgun E, Uyar T (2016) Quercetin/β-cyclodextrin inclusion complex embedded nanofibres: slow release and high solubility. Food Chem 197:864–871

[12] Agarwal S, Wendorff JH, Greiner A (2008) Use of electrospinning technique for biomedical applications. Polymer 49:5603–5621

[13] Bhardwaj N, Kundu SC (2010) Electrospinning: a fascinating fiber fabrication technique. Biotechnol Adv 28:325–347

[14] Uyar T, Kny E (eds) (2017) Electrospun materials for tissue engineering and biomedical applications: research, design and commercialization, 1st edn. Woodhead Publishing, Cambridge

[15] Celebioglu A, Kayaci-Senirmak F, Ipek S, Durgun E, Uyar T (2016) Polymer-free nanofibers from vanillin/cyclodextrin inclusion complexes: high thermal stability, enhanced solubility and antioxidant property. Food Funct 7(7):3141–3153

[16] Uyar T, Hacaloglu J, Besenbacher F (2011) Electrospun polyethylene oxide (PEO) nanofibers containing cyclodextrin inclusion complex. J Nanosci Nanotechnol 11(5):3949–3958

[17] Li XY, Shi CJ, Yu DG, Liao YZ, Wang X (2014) Electrospun quercetin-loaded zein nanoribbons. Bio Med Mater Eng 24(6):2015–2023

[18] Thipkaew C, Wattanathorn J, Muchimapura S (2017) Electrospun nanofibers loaded with quercetin promote the recovery of focal entrapment neuropathy in a rat model of streptozotocin-induced diabetes. BioMed Res Int 2017493, 12

[19] Li XY, Li YC, Yu DG, Liao YZ, Wang X (2013) Fast disintegrating quercetin-loaded drug delivery systems fabricated using coaxial electrospinning. Int J Mol Sci 14(11):21647–21659

[20] Kohn W, Sham LJ (1965) Self-consistent equations including exchange and correlation effects. Phys Rev 140(4A):A1133–A1138

[21] Hohenberg P, Kohn W (1964) Inhomogeneous electron gas. Phys Rev 136(3B):B864–B871

[22] Kresse G, Furthmüller J (1996) Efficient iterative schemes for ab initio total-energy calculations using a plane-wave basis set. Phys Rev B 54(16):11169–11186

[23] Kresse G, Furthmüller J (1996) Efficiency of ab initio total energy calculations for metals and semiconductors using a plane-wave basis set. Comput Mater Sci 6(1):15–50

[24] Perdew JP, Chevary JA, Vosko SH, Jackson KA, Pederson MR, Singh DJ, Fiolhais C (1992) Atoms, molecules, solids, and surfaces: applications of the generalized gradient approximation for exchange and correlation. Phys Rev B 46(11):6671–6686

[25] Grimme S (2006) Semiempirical GGA-type density functional constructed with a long-range dispersion correction. J Comput Chem 27(15):1787–1799

[26] Blöchl PE (1994) Projector augmented-wave method. Phys Rev B 50(24):17953–17979

[27] Allen FH (2002) The Cambridge structural database: a quarter of a million crystal structures and rising. Acta Crystallogr B 58(3):380–388

[28] Fattebert JL, Gygi F (2003) First-principles molecular dynamics simulations in a continuum solvent. Int J Quant Chem 93(2):139–147

[29] Andreussi O, Dabo I, Marzari N (2012) Revised self-consistent continuum solvation in electronic-structure calculations. J Chem Phys 136(6):064102–064120

[30] Petrosyan SA, Rigos AA, Arias TA (2005) Joint density-functional theory: ab initio study of Cr_2O_3 surface chemistry in solution. J Phys Chem B 109(32):15436–15444

[31] Mathew K, Sundararaman R, Letchworth-Weaver K, Arias TA, Hennig RG (2014) Implicit solvation model for density-functional study of nanocrystal surfaces and reaction pathways. J Chem Phys 140(8):084106–084108

[32] Tang P, Li S, Wang L, Yang H, Yan J, Li H (2015) Inclusion complexes of chlorzoxazone with β-and hydroxypropyl-β-cyclodextrin: characterization, dissolution, and cytotoxicity. Carbohydr Polym 131:297–305

[33] Borghetti GS, Lula IS, Sinisterra RD, Bassani VL (2009) Quercetin/β-Cyclodextrin solid complexes prepared in aqueous solution followed by spray-drying or by physical mixture. AAPS PharmSciTech 10(1):235–242

[34] Ali S, Khatri Z, Oh KW, Kim IS, Kim SH (2014) Zein/cellulose acetate hybrid nanofibers: electrospinning and characterization. Macromol Res 22(9):971–977

[35] Aytac Z, Ipek S, Durgun E, Tekinay T, Uyar T (2017) Antibacterial electrospun zein nanofibrous web encapsulating thymol/cyclodextrin-inclusion complex for food packaging. Food Chem 233:117–124

[36] Aytac Z, Kusku SI, Durgun E, Uyar T (2016) Encapsulation of gallic acid/cyclodextrin inclusion complex in electrospun polylactic acid nanofibers: release behavior and antioxidant activity of gallic acid. Mater Sci Eng, C 63:231–239

[37] Uyar T, Hunt MA, Gracz HS, Tonelli AE (2006) Crystalline cyclodextrin inclusion compounds formed with aromatic guests: Guest-dependent stoichiometries and hydration-sensitive crystal structures. Cryst Growth Des 6:1113–1119

[38] Kayaci F, Sen HS, Durgun E, Uyar T (2014) Functional electrospun polymeric nanofibers incorporating geraniol–cyclodextrin inclusion complexes: high thermal stability and enhanced durability of geraniol. Food Res Int 62:424–431

[39] Celebioglu A, Uyar T (2011) Electrospinning of polymer-free nanofibers from cyclodextrin inclusion complexes. Langmuir 27(10):6218–6226

[40] Neo YP, Ray S, Jin J, Gizdavic-Nikolaidis M, Nieuwoudt MK, Liu D, Quek SY (2013) Encapsulation of food grade antioxidant in natural biopolymer by electrospinning technique: a physicochemical study based on zein-gallic acid system. Food Chem 136(2):1013–1021

[41] Uyar T, Besenbacher F (2008) Electrospinning of uniform polystyrene fibers: the effect of solvent conductivity. Polymer 49(24):5336–5343

[42] Brand-Williams W, Cuvelier ME, Berset CLWT (1995) Use of a free radical method to evaluate antioxidant activity. LWT Food Sci Technol 28(1):25–30